

See discussions, stats, and author profiles for this publication at: <https://www.researchgate.net/publication/241701493>

Solvent Effects on the UV-vis Absorption and Emission of Optoelectronic Coumarins: a Comparison of Three Empirical Solvatochromic Models

ARTICLE *in* THE JOURNAL OF PHYSICAL CHEMISTRY C · JUNE 2013

Impact Factor: 4.77 · DOI: 10.1021/jp310397z

CITATIONS

14

READS

60

3 AUTHORS, INCLUDING:



Xiaogang Liu

Singapore-MIT Alliance for Research and Tech...

17 PUBLICATIONS 372 CITATIONS

SEE PROFILE

Solvent Effects on the UV–vis Absorption and Emission of Optoelectronic Coumarins: a Comparison of Three Empirical Solvatochromic Models

Xiaogang Liu,[†] Jacqueline M. Cole,^{*,†,‡,§} and Kian Sing Low[†]

[†]Cavendish Laboratory, Department of Physics, University of Cambridge, J. J. Thomson Avenue, Cambridge, CB3 0HE United Kingdom

[‡]Department of Chemistry, University of New Brunswick, P.O. Box 4400, Fredericton, NB, E3B 5A3 Canada

[§]Department of Physics, University of New Brunswick, P.O. Box 4400, Fredericton, NB, E3B 5A3 Canada

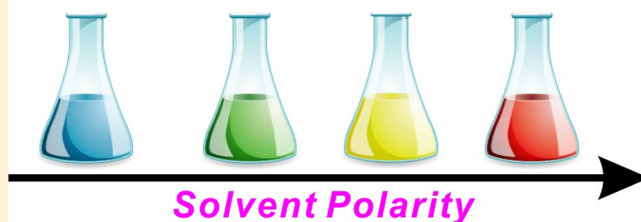
S Supporting Information

ABSTRACT: Coumarins often function in the solution phase for a diverse range of optoelectronic applications. The associated solvent effects on the UV–vis absorption and/or fluorescence spectral shifts of coumarins need to be understood in order that their photochemistry can be controlled. To this end, three different empirical solvatochromic models are assessed against 13 coumarins. The two generalized solvent scales developed by Catalán and co-workers demonstrate comparable performance to the popular Taft–Kamlet solvatochromic comparison method. A combinatorial approach to determine the best-fit equations in all of the empirical models is applied; this involves both statistical best-fits and the physical validation of the resulting parameters, based on the molecular structures of solvents and solutes and their corresponding interactions. The findings of this approach are used to extract useful information about different aspects of solvent effects on the solvatochromism of coumarins.

Empirical Solvatochromic Models

Taft–Kamlet Model

Catalán Models



1. INTRODUCTION

Solvent effects play an important role in the optoelectronic properties of coumarin dyes, which mainly function in the solution phase. Understanding these solvent effects is essential in order to comprehend the complex photophysics and photochemistry of coumarins. To this end, it has been shown that there is a heavy reliance of solvatochromism on interpreting solvent effects in coumarins.¹ In these studies, coumarins are dissolved into a number of different solvents, and the shifts of their peak UV–vis absorption/fluorescence wavelengths (λ_{max}) are exploited in order to extract useful information; for instance, the dipole moments of coumarins in both their ground and excited states,^{1c,d} the flip-flop motions of some coumarin substituents in nonpolar solvents,^{1e–h} and the formation of hydrogen bonds between coumarins and solvent molecules.¹ⁱ Solvatochromic studies also allow one to decouple the λ_{max} shifts into different categories, such as nonspecific and specific solvent effects. By a nonspecific solvent effect, we mean that the solvent acts as a continuous and uniform dielectric. In contrast, specific solvent effects concern a directional, nonuniform distribution of the molecular-level interactions between solvents and solutes, such as hydrogen bond interactions.²

The most popular solvatochromic model currently in use is probably the Taft–Kamlet solvatochromic comparison method.³ In this model, multiple parameters are deployed in order to

characterize different solvent–solute interactions, in the form of eq 1.³

$$\nu = \nu_0 + s(\pi^* + d\delta) + a\alpha + b\beta \quad (1)$$

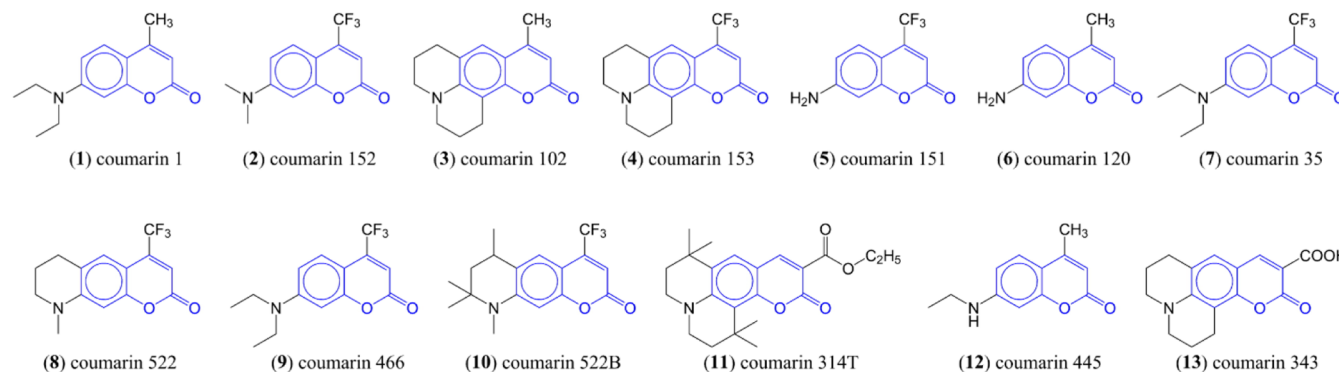
$$\nu = \nu_0 + s\pi^* + a\alpha + b\beta, \quad \text{when } d = 0 \quad (2)$$

In this equation, ν represents the transition energy (or the reciprocal of λ_{max}) and ν_0 is its value in cyclohexane. π^* , α , and β describe the solvent polarity (which refers to dipolarity and polarizability jointly), solvent hydrogen-bond donor (HBD) acidity (the ability of the solvent to donate a proton to a solvent-to-solute hydrogen bond), and solvent hydrogen-bond acceptor (HBA) basicity (the ability of the solvent to accept a proton from a solvent-to-solute hydrogen bond). δ is a correction term introduced on account of different polarizability of aromatic and polychlorinated solvents with respect to aliphatic and nonpolychlorinated solvents; it is set to 0 for nonchloro-substituted aliphatic solvents, 0.5 for polychlorinated aliphatics, and 1 for aromatic solvents.^{3d} When the spectra of the solute have a red shift as the solvent polarity increases (namely positive solvatochromism), such as in the case of coumarins, this

Received: October 19, 2012

Revised: May 19, 2013

Published: June 18, 2013

Scheme 1. Molecular Structures of Coumarins 1, 152, 102, 153, 151, 120, 35, 522, 466, 522B, 314T, 445, and 343 (1–13)^a

^aTheir common coumarin fragment is highlighted in blue.

correction term is not required, and its coefficient, d , should be set to 0.^{3d} As a result, eq 1 can be reduced into eq 2.

These solvent properties, π^* , α , and β , are typically determined from the solvent-induced λ_{\max} shifts of several probe dyes. Their respective coefficients, s , a , and b quantify the contributions from these distinctive solvent properties upon a change in ν . Furthermore, the solvent property scales in the Taft–Kamlet model are normalized such that the ratios between their coefficients quantify their relative contributions.^{3d} Moog et al.^{1a,b} have shown that the Taft–Kamlet model offers excellent performance in describing the solvatochromism of coumarins, superior to another two commonly used models: the reaction field approach⁴ and the $E_T(30)$ polarity scale based method.⁵ This is because the latter two methods exclude, or treat incompletely, the specific solvent effect.

Another relatively recent model, the generalized model, has been proposed by Catalán and co-workers.⁶ In this model, Catalán has constructed new scales for solvent polarity (SPP), solvent acidity (SA), and solvent basicity (SB), as analogues of π^* , α , and β . These new scales have been formulated in response to some contamination of Taft–Kamlet's scales, due to the mixing of both specific and nonspecific effects in some solvent parameters,⁷ and their relatively poor performance in nonpolar and less polarized solutes.⁸ More importantly, it is argued that one should always adjust the solvent scales using homomorphs of the probe dyes in order to remove or minimize contaminations. A homomorph has a very similar molecular structure and optical excitation mechanism to the probe dye but different sensitivity to a particular solvent property which is intended for study. Consequently, one can subtract the transition energies of the homomorph from those of the probe dye in order to cancel out any spurious effects, and the remaining differences are purely attributed to that distinct solvent property. These values can then be used to construct solvent property scales.^{6a} Catalán's SPP, SA and SB scales lead to a similar expression as to eq 2. In this paper, we refer to it as the Catalán3P model (eq 3; 3P refers to the three parameters involved in this model).

More recently, the polarity scale (SPP) has been further separated into two parameters: solvent polarizability (SP) and dipolarity (SdP) scales.^{6d} This separation is based on the data of two probe dyes: 3,20-di(*tert*-butyl)-2,2,21,21-tetramethyl-all-*trans*-3,5,7,9,11,13,15,17,19-docosanonaen ("ttbP9") and 2-(dimethyl-amino)-7-nitrofluorene ("DMANF").^{6d} The former responds exclusively to the polarizability of the medium, and the latter is sensitive to both solvent dipolarity and polarizability. With this split, a more generalized model, denoted as the

Catalán4P model in this paper, is introduced (eq 4).^{6d} It has been demonstrated that Catalán4P offers better statistics when describing the solvatochromism of a few boron-dipyrromethene ("BODIPY") dyes,⁹ in comparison to the Taft–Kamlet model.

$$\nu = \nu_0 + c_{\text{spp}}\text{SPP} + c_{\text{sa}}\text{SA} + c_{\text{sb}}\text{SB} \quad (3)$$

$$\nu = \nu_0 + C_{\text{SP}}\text{SP} + C_{\text{SdP}}\text{SdP} + C_{\text{SA}}\text{SA} + C_{\text{SB}}\text{SB} \quad (4)$$

Given that the interpretation of solvatochromism results is highly influential in analyzing the solvent effects, a detailed enquiry into solvatochromism effects on coumarins is herein performed. In the first instance, we extend the work of Moog et al.^{1a,b} and compare the performance of the Taft–Kamlet and Catalán models in describing the solvatochromism of a series of 13 coumarins shown in Scheme 1. Second, the associated coumarin data are employed in order to gain a deeper understanding about solvent-coumarin interactions, by analyzing information derived from the appropriate solvatochromic models.

Within this scope, the UV–vis peak absorption wavelengths of these coumarins in ~18 different solvents are fitted into both the Taft–Kamlet and the Catalán models, in order to evaluate their relative performance, and elucidate the nature of solvent-coumarin interactions. These coumarins contain different HBA and HBD moieties. Their solute–solvent interactions thus cover different aspects of specific solvent effects, while the nonspecific solvent effects are ubiquitous for all coumarins. Furthermore, these UV–vis absorption and fluorescence data are compiled from various sources and measured in different types of solvents. Both the UV–vis absorption and emission data of 1–9 are imported from the literature,^{1b,e,10} and the absorption data of 10–13 are measured in-house. While some groups have intentionally avoided using chlorinated and aromatic solvents, others do not limit their choice of solvents. Hence, the compiled spectral data also allows us to assess the choice of solvents on the performance of the empirical solvatochromic models. While the solvent effects on coumarins underlie our motivation for this study, it is expected that the overall results are highly relevant to all solvent-effect investigations in general; as such, they could be applicable to a wide range of chemical compounds.

2. EXPERIMENTAL METHODS AND DATA SELECTION

2.1. UV–vis Absorption and Fluorescence Transition Energies. The transition energies of both UV–vis absorption and fluorescence for 1–9 were imported from the literature.^{1b,e,10} For the same coumarins, only data from a single source

were used. We did not combine data reported in different papers, in order to avoid systematic instrument shift caused errors. In particular, the data of 1, 4, and 5 were each reported by two different teams, using different sets of solvents and different techniques to calculate the transition energies (sections 3.2 and 3.3).^{1b,e,10} Both sets of data for these three coumarins were imported and analyzed.

The $\lambda_{\text{max}}^{\text{abs}}$ values of 10–13 were measured in-house using materials supplied by the Exciton chemical company. The data of 10–12 were measured in seventeen solvents: acetone, acetonitrile, cyclohexane, diethyl ether, ethanol, ethyl acetate, ethylene glycol, methanol, propan-2-ol, chloroform, dichloromethane, dimethyl sulfoxide (DMSO), 1-hexanol, *n*-pentane, pyridine, tetrahydrofuran, and toluene. All of these seventeen solvents had a purity higher than 99.5%. Dilute solution samples ($\sim 10^{-5}$ M; with absorption below 10% of the incident light) were tested on a Hewlett-Packard G1103A spectrophotometer.

The $\lambda_{\text{max}}^{\text{abs}}$ values of 13 were measured only in the first 9 solvents listed above as well as in deionized water, using the same method and setup. The uncertainties in all our $\lambda_{\text{max}}^{\text{abs}}$ readings are ± 1 nm.

2.2. Data Selection. The UV–vis absorption/fluorescence spectral data are subdivided into three sets, based on the method used to deduce the transition energies, ν , and the types of solvents in use, as illustrated in Figure 1 and Table 1.

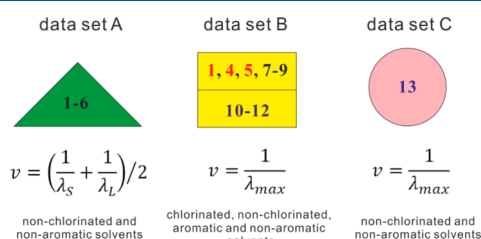


Figure 1. Classification of data sets A–C.

Table 1. Numbers of Solvents in Use for Data Sets A–C^a

compound	number of nonaromatic and nonchlorinated solvents	number of aromatic and polychlorinated solvents	total sample size
data set A			
1–6	18	0	18
data set B			
1 and 9	14	6	20
4, 7, and 8	13	3	16
5	16	0	16
10–12	13	4	17
data set C			
13	10	0	10

^aFor compounds 1–9, both UV–vis absorption and fluorescence data were imported from the literature. For compounds 10–13, only the UV–vis absorption data were measured in-house. See the Supporting Information for further details.

In the first set (or data set A), the spectral data of 1–6 are imported from the work of Moog et al.^{1b} Moog and co-workers define the transition energy as

$$\nu = \left(\frac{1}{\lambda_S} + \frac{1}{\lambda_L} \right) / 2 \quad (5)$$

where λ_S and λ_L correspond, respectively, to the shorter and longer wavelengths at which the UV–vis absorption/fluorescence is equal to half of its peak spectral intensity. Calculating the transition energy in this way takes into account changes in the band shapes of coumarins that may occur when they are dissolved into different solvents. Conversely, the exclusive use of the reciprocal of λ_{max} to calculate ν in different solvents is less representative of the same relative position within the absorption profiles.^{1a,b}

Furthermore, it should be pointed out that aromatic and polychlorinated solvents, whose polarizability is relatively different from that of aliphatic and nonpolychlorinated solvents, are excluded from Moog's experiments.

In the second set (data set B), the transition energies, ν , are derived by just taking the reciprocal of λ_{max} . Furthermore, this assessment employed UV–vis absorption and/or fluorescence data originating from researchers other than Moog et al., imported both from the literature (for 1, 4, 5, and 7–9),^{1e,10} and our in-house measurements (for 10–12). Aromatic and polychlorinated solvents are included in these data.

In particular, since 1, 4, and 5 appear in both data sets A and B, a cross-check of their fitting parameters to the empirical solvatochromic models allows one to directly assess the impact of solvent selection and the method of calculating ν on the overall performance of the solvatochromic models.

In the last set (data set C), the transition energies of 13, which are derived by taking the reciprocal of λ_{max} in ten nonchlorinated and nonaromatic solvents, are used to illustrate the impact of other non-hydrogen bonding types of specific solvent effects, which are not accounted for in the three empirical solvatochromic models.

3. RESULTS AND DISCUSSION

3.1. Statistical and Physical Criteria Used to Evaluate the Performance of Empirical Solvatochromic Models.

The ν of 1–13 in ~ 17 solvents are fitted using three empirical solvatochromic models: the Taft–Kamlet, the Catalán3P, and Catalán4P models. The objectives of this solvatochromic study were 2-fold: (1) evaluate the relative performance of the three empirical models and (2) study the solvent effects on the spectral shifting of 1–13. These objectives were achieved via two steps: first, the fitting of ν to the solvatochromic models was performed purely statistically; second, their physical validity was checked, according to solvent–solute interactions.

For the statistical fitting of ν , a multiple linear regression method was used to determine the coefficients of the solvatochromic parameters (eqs 2–4). In addition, *F*-statistics were applied to include only statistically significant parameters in the final best-fits. *F*-statistics essentially determine how many parameters in the solvatochromic models are required to explain most of the variance in ν . A detailed implementation of *F*-statistics has been introduced by the work of Moog et al.^{1b} and is summarized herein.

The *F*-number (in the *F*-statistics) is defined as

$$F \equiv \frac{[\text{SS}(\text{data}) - \text{SS}(\text{fit})]/(p - 1)}{\text{SS}(\text{fit})/(n - p)} \quad (6)$$

where *n* is the sample size, *p* the number of parameters to fit, and

$$\text{SS}(\text{data}) = \sum_i (v_i^{\text{obs}} - \bar{v}^{\text{obs}})^2 \quad (7)$$

$$SS(\text{fit}) = \sum_i (\nu_i^{\text{obs}} - \nu_i^{\text{fit}})^2 \quad (8)$$

where ν_i^{obs} and ν_i^{fit} represent the transition energy from experimental observations and statistical fits, respectively, and $\bar{\nu}^{\text{obs}}$ is the average observed transition energy.

During the multiple linear regressions, a number of cases, including different combinations of the solvatochromic parameters, were considered. For example, for the Catalán4P model, 17 cases were considered in total: 4 cases, each including only one of the four parameters (SP, SdP, SA, and SB); 6 cases, each including two of the four parameters; 4 cases, each including three of the four parameters; and the last case, including all the four parameters in the fitting. The *F*-number was calculated for all these 17 cases, and the one with the highest *F*-number was considered as the statistical best-fit.

The best-fits of the three solvatochromic models used a different number of parameters. Including more parameters almost always improves the statistical correlation coefficient, *r*. To counter this bias and make a fair comparison, the goodness-of-fit was quantified by an adjusted *R*² figure-of-merit (adj *R*², eq 9) when these models are compared.^{1b} The adj *R*² penalizes a model for using more parameters and it is always lower than *r*.

$$\text{adj}R^2 = 1 - \frac{SS(\text{fit})(n-1)}{SS(\text{data})(n-p)} \quad (9)$$

The physical origin of these fitted parameters was then examined, based on the nature of solvent–solute interactions. Nonspecific solvent effects are always present. They stabilize coumarins through solvent–coumarin dipole–dipole interactions, or induced dipole–dipole interactions. The dipole moments of coumarins increase upon excitation.¹¹ This solvent stabilization effect therefore results in the corresponding reduction of the excited state energy levels relative to those of the ground states. Consequently, an overall red shift is expected as coumarins are dissolved into solutions; and a decreasing energy gap becomes more significant as the solvent polarity rises. This trend should be captured by negative coefficients, *s*, *c*_{SPP}, *C*_{SP}, and/or *C*_{SdP}, that are associated with the nonspecific solvent properties, π^* , SPP, SP, and SdP, in all three solvatochromic models.

Moving on to investigate the specific solvent effect, intermolecular hydrogen-bonds were considered at the molecular level. Common types of hydrogen bonds between coumarins and solvents are illustrated in Figure 2, using **12** and **13** as examples. In coumarins, the nitrogen atom is able to act as a hydrogen-bond acceptor (HBA) by donating its lone pair, forming a type A hydrogen bond with a hydrogen-bond donor (HBD) solvent. Similarly, the carbonyl oxygen participates in type B hydrogen bonding with a HBD solvent. Type A bonding results in a blue shift of coumarin spectra, versus a red shift

caused by type B bonding. This is due to their opposing effects on coumarin intramolecular charge transfer (ICT).¹² Nevertheless, type B bonding usually has a more significant role, as reflected by a net red shift in HBD solvents.^{1b} Since both type A and B hydrogen bonds are common to all coumarins **1–13**, the coefficients, *a*, *c*_{SA}, and *C*_{SA}, associated with the solvent acidity (α or SA), are expected to be negative in all best-fits.

In **5**, **6**, **12**, and **13**, hydrogen atoms attached to either N or O atoms function as HBDs and form type C or D hydrogen bonds in the presence of HBA solvents. Since type C and D bonds are present only in these four coumarins, the solvent basicity coefficients, *b*, *c*_{SB}, and *C*_{SB}, which are associated with β or SB, are expected to be nonzero exclusively for these four coumarins, and to be null for all remaining coumarins.

In **11** and **13**, other types of intermolecular hydrogen bonds also exist, owing to the presence of O atoms at the –COOR (*R* = H, CH₃) group. Since these hydrogen bonds boost ICT, a corresponding reduction in transient energies is expected. Their effects have been accounted for implicitly in *a*, *c*_{SA}, and *C*_{SA}, the negative coefficients of α and SA.

3.2. Evaluation of the Solvatochromic Models for **1–6** Based on Moog's Approach (Data Set A).

With Moog's approach, the transition energies of **1–6** are determined via eq 5 in 18 nonchlorinated and nonaromatic solvents. Calculating the transition energy in this way, rather than directly using the reciprocal of λ_{max} , takes into consideration of possible changes of the band shapes of coumarins when they are dissolved into different solvents.^{1a,b} In addition, aromatic and polychlorinated solvents, whose polarizability is relatively different from that of aliphatic and nonpolychlorinated solvents, are excluded from data set A.

However, slightly different solvent parameters in the Taft–Kamlet model were used in our treatment: a comprehensive review of the Taft–Kamlet solvent properties was first given by Kamlet et al. in 1983.^{3d} A revised version was released by Marcus in 1993.¹³ In both of these versions, the π^* scale was determined based on the averaged results from a number of probe dyes. It was believed that in this manner, anomalies related to any single probe dye would be canceled out, leading to more accurate results.^{3a–c} Laurence et al. also introduced a revised π^* scale, based on UV–vis spectra of only two probe dyes: 4-nitroanisole and *N,N*-dimethyl-4-nitroaniline for good reasons.¹⁴ However, in their scales, only nonprotonic solvents were included; the π^* values for protonic solvents, such as those of alcohols, have not been defined yet. The differences among these π^* polarity scales are essentially caused by a different mixture of dipolarity and polarizability, owing to different choices of probe dyes.² After a critical examination of these π^* scales, Abboud et al. concluded that it was up to the reader to choose the preferred scale.¹⁵ In Moog's work, the solvent parameters had mixed origins; that is, those defined by Kamlet et al. were in use, except for the π^* values for nonprotonic solvents, where Laurence's parameters were adopted. We, however, prefer to use the more updated results compiled by Marcus; and for consistency all π^* values in use herein are those obtained by averaging data from multiple probe dyes.

Based on data set A (Supporting Information) and applying relevant solvent properties defined by the three solvatochromic models (Supporting Information), the best-fit parameters for each empirical solvatochromic model were calculated, as summarized in Table 2.

Statistically, the Taft–Kamlet model, the Catalán3P model and the Catalán4P model all demonstrate excellent performance,

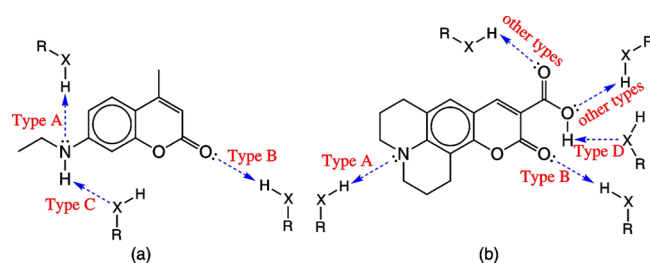


Figure 2. Four classification types of hydrogen bonds in coumarins.

Table 2. Statistical Best-Fit Parameters ($\times 10^3 \text{ cm}^{-1}$) of the Empirical Solvatochromic Models for Data Set A^a

	Taft–Kamlet model					Catalán3P model					Catalán4P model				
	ν_0	s	a	b	adj R^2	ν_0	ϵ_{app}	ϵ_{sa}	ϵ_{sb}	adj R^2	ν_0	C_{SP}	C_{SAP}	C_{SA}	adj R^2
1 (abs)^b	28.61 (0.11)	-1.37 (0.20)	-0.82 (0.18)		0.954	30.21 (0.33)	-2.94 (0.43)	-1.24 (0.37)		0.958	29.93 (0.74)	-2.07 (1.12)	-1.03 (0.19)	-1.42 (0.41)	0.961
1 (flu)^c	25.43 (0.16)	-2.94 (0.28)	-1.99 (0.25)		0.982	28.88 (0.50)	-6.30 (0.66)	-3.10 (0.56)		0.980	25.41 (0.19)		-2.56 (0.31)	-2.71 (0.67)	0.973
2 (abs)	27.07 (0.10)	-1.45 (0.23)	-0.38 (0.20)	-0.47 (0.31)	0.975	29.09 (0.24)	-3.76 (0.31)	-0.63 (0.27)		0.981	28.69 (0.47)	-2.44 (0.70)	-1.16 (0.14)	-0.69 (0.26)	0.987
2 (flu)	23.41 (0.23)	-3.95 (0.53)	-1.49 (0.44)	-1.05 (0.70)	0.983	28.74 (0.57)	-9.91 (0.75)	-2.42 (0.65)		0.986	24.66 (1.06)	-1.75 (1.59)	-3.50 (0.31)	-1.72 (0.59)	0.991
3 (abs)	27.68 (0.12)	-1.34 (0.20)	-1.00 (0.18)		0.958	29.27 (0.37)	-2.90 (0.48)	-1.55 (0.41)		0.953	27.67 (0.15)		-1.16 (0.24)	-1.39 (0.51)	0.931
3 (flu)	24.53 (0.19)	-3.00 (0.33)	-2.04 (0.29)		0.976	28.06 (0.60)	-6.45 (0.79)	-3.14 (0.68)		0.972	24.52 (0.21)		-2.63 (0.33)	-2.73 (0.72)	0.971
4 (abs)	25.47 (0.12)	-1.69 (0.22)	-0.66 (0.19)		0.956	27.49 (0.29)	-3.67 (0.37)	-0.81 (0.32)		0.974	27.21 (0.59)	-2.58 (0.89)	-1.15 (0.17)	-0.92 (0.33)	0.980
4 (flu)	22.01 (0.19)	-3.81 (0.34)	-1.69 (0.30)		0.979	26.58 (0.45)	-8.30 (0.60)	-2.16 (0.51)		0.987	23.28 (1.02)	-1.67 (1.52)	-2.94 (0.29)	-1.65 (0.57)	0.989
5 (abs)	29.17 (0.09)	-0.81 (0.19)		-2.81 (0.20)	0.992	31.12 (0.37)	-3.38 (0.56)	-0.76 (0.41)	-1.99 (0.32)	0.986	31.09 (0.60)	-2.74 (0.90)	-1.05 (0.17)	-0.94 (0.34)	0.992
5 (flu)	24.64 (0.19)	-3.04 (0.44)	-1.19 (0.37)	-2.13 (0.58)	0.988	28.95 (0.46)	-7.71 (0.71)	-2.15 (0.52)	-1.56 (0.41)	0.991	25.88 (0.98)	-1.65 (1.47)	-2.87 (0.28)	-1.79 (0.55)	0.992
6 (abs)	30.68 (0.14)	-0.69 (0.34)	-0.35 (0.27)	-1.81 (0.44)	0.972	32.14 (0.50)	-2.55 (0.77)	-1.04 (0.56)	-1.32 (0.43)	0.960	32.67 (0.88)	-2.90 (1.32)	-0.67 (0.27)	-1.36 (0.50)	0.977
6 (flu)	26.50 (0.13)	-1.87 (0.29)	-1.42 (0.25)	-1.57 (0.39)	0.990	29.13 (0.49)	-4.69 (0.75)	-2.74 (0.55)	-1.27 (0.43)	0.983	26.60 (0.20)		-1.81 (0.32)	-2.37 (0.61)	0.980
mean					0.976					0.976					0.977

^aThe numbers in parentheses represent 95% confidence limits for their corresponding fitting coefficients. Physically invalid terms (based on coumarin-solvent interactions) and dubious terms (with very larger uncertainty values) are highlighted in bold. ^b"abs" refers to the UV-vis absorption data. ^c"flu" refers to the fluorescence data.

Table 3. Selected Fitting Results to the Absorption Data of **2** When Different Combinations of Solvent Properties Are Included in the Best-Fits^a

Taft–Kamlet model						
ν_0	s	a	b	F	adj R^2	
27.07 (0.10)	−1.45 (0.23)	−0.38 (0.20)	−0.47 (0.31)	224	0.975	
27.01 (0.12)	−1.71(0.21)	−0.59(0.18)		201	0.959	
27.10(0.14)	−1.25 (0.31)		−0.89(0.32)	155	0.948	
26.92 (0.22)	−1.80 (0.40)			90	0.839	
Catalán3P model						
ν_0	c_{spp}	c_{sa}	c_{sb}	F	adj R^2	
29.09 (0.24)	−3.76 (0.31)	−0.63 (0.27)		442	0.981	
29.22 (0.37)	−4.02 (0.46)			343	0.953	
29.04 (0.24)	−3.61 (0.38)	−0.58 (0.27)	−0.15 (0.22)	318	0.982	
29.10 (0.37)	−3.69 (0.56)		−0.28 (0.31)	203	0.960	
Catalán4P model						
ν_0	C_{SP}	C_{SDP}	C_{SA}	C_{SB}	F	adj R^2
28.69 (0.47)	−2.44 (0.70)	−1.16 (0.14)	−0.69 (0.26)	−0.42 (0.18)	332	0.987
27.00 (0.17)		−1.57 (0.24)			185	0.915
28.49 (0.78)	−2.28 (1.17)	−1.33 (0.19)	−0.81 (0.43)		152	0.964
28.21 (0.77)	−1.67 (1.14)	−1.28 (0.23)		−0.52 (0.31)	134	0.959
27.10 (0.17)		−1.38 (0.27)		−0.43 (0.38)	123	0.935
27.85 (0.98)	−1.30 (1.49)	−1.52 (0.23)			109	0.927
27.00 (0.16)		−1.48 (0.26)	−0.44 (0.55)		105	0.924
27.08 (0.17)		−1.35 (0.28)	−0.31 (0.53)	−0.37 (0.39)	86	0.937

^aAll fitting parameters are in units of 10^3 cm^{-1} . The physically valid best-fits are highlighted in italics.

with adj R^2 averaged at 0.976 (or 0.985 if using Moog's Taft–Kamlet solvent parameters), 0.976, and 0.977, respectively.¹⁶ Their goodness-of-fits are comparable with each other.

Physically, the best-fit results are reasonable in most cases. For example, all the models have successfully predicted the negative coefficients associated with π^* , SPP, SP, and/or SDP, suggesting an overall red shift of coumarins as solvent polarity increases; negative coefficients associated with α and SA are present in all cases but one, indicating that all coumarins, perhaps except one, are able to act as HBAs and resulting coumarin–solvent interactions cause the reduction of transition energies. Furthermore, in the Catalán3P model, the negative coefficients of SB revealed for **5** and **6** and the null terms for the remaining coumarins **1–4** clearly suggest that the interactions between coumarins and HBA solvents are present only in **5** and **6**, but not in **1–4**. These results are in accordance with the molecular structures of **1–6**, i.e., only **5** and **6** contain HBD moieties among these six coumarins (see Scheme 1).

Nevertheless, there are also a few unexpected terms (b and C_{SB} , associated with β and SB) in the best-fit equations derived from the Taft–Kamlet and Catalán4P models, as highlighted in bold in Table 2. In the Taft–Kamlet model, the nonzero values of b in the best-fits of **2** predict the presence of a HBD moiety in this compound, while one does not exist. The presence of physically invalid terms in this model has also been reported previously.^{1b,i} This type of failure appears more frequent in the Catalán4P model, which suggests that both **2** and **4** are HBDs; this is clearly invalid based on their molecular structures (Scheme 1).

The presence of these invalid terms in the statistical best-fits can be probably rationalized by considering more extensive fitting results to the UV–vis absorption data of **2** (Table 3). For the same set of data, considerably different fitting equations can be achieved, which all lead to very decent goodness-of-fit statistics for all three empirical models. This problem is particularly serious for the Catalán4P model, since it includes

one more parameter than the other two models. The physically valid best-fit (shown in italics in Table 3) does not necessarily have the highest F -number among all fitting results, as shown in the case of the Taft–Kamlet model (with the second highest F -number), and the Catalán4P model (with the third highest F -number). Therefore, care must be taken when selecting the best-fit.

In contrast, statistical analysis in combination with physical validations (based on actual solvents–solution interactions) leads to more reliable results. We therefore extended the approach of Moog et al. by forcing the unphysical terms in the best-fits to null, which afforded the revised parameters in Table 4. (A complete version of the revised table can be found in the Supporting Information; Table S4). This constraint imposition circumvents various problems associated with the three solvatochromic models. For example, in the fluorescence data of **5**, the fitting equation in the Catalán4P model appears dubious (Table 2). Its coefficient C_{SP} has a very large uncertainty value, in contrast to the null values in the best-fits of the remaining fluorescence data (Table 4). Revised parameters for this case, by setting C_{SP} to 0, are also reported (Table 4). It is worth highlighting that with these modifications by constraint, the adj R^2 for all of the three solvatochromic models remain very high (Table 4; Supporting Information: Table S4), averaging 0.973 (for the Taft–Kamlet model), 0.976 (for the Catalán3P model), and 0.971 (for the Catalán4P model), respectively; in addition, the revised best-fit parameters are all physically valid in predicting the red/blue spectral shifts owing to different aspects of the solvent effects, i.e., in accordance with the physical criteria outlined in section 3.1.

The best-fit equations for the solvatochromic models also allow one to predict the transition energies of coumarins in vacuo via interpolation (Table 5). These energies in vacuo given by different models agree reasonably well, particularly for the absorption data where the average difference amounted to $0.83 \times 10^3 \text{ cm}^{-1}$. However, relatively large differences averaging to 4.25

Table 4. Revised Best-Fit Parameters ($\times 10^3 \text{ cm}^{-1}$) of the Empirical Solvatochromic Models for Data Set A^a

	Taft–Kamlet model				
	ν_0	s	a	b	adj R^2
2 (abs)	27.01 (0.12)	−1.71 (0.21)	−0.59 (0.18)		0.959
2 (flu)	23.28 (0.26)	−4.53 (0.46)	−1.95 (0.41)		0.973
	Catalán4P model				
	ν_0	C_{SP}	C_{SdP}	C_{SA}	adj R^2
2 (abs)	28.49 (0.78)	−2.28 (1.17)	−1.33 (0.19)	−0.81 (0.43)	0.964
2 (flu)	23.28 (0.27)		−4.02 (0.43)	−1.81 (0.93)	0.972
4 (abs)	27.05 (0.76)	−2.45 (1.15)	−1.29 (0.19)	−1.02 (0.42)	0.966
4 (flu)	22.01 (0.23)		−3.36 (0.36)	−1.66 (0.78)	0.972
5 (flu)	24.79 (0.19)		−3.00 (0.30)	−1.53 (0.57)	0.990

^aThe numbers in parentheses represent 95% confidence limits for their corresponding fitting coefficients; unphysical fitting parameters have been constrained to 0.

Table 5. Projected Transition Energies ν ($\times 10^3 \text{ cm}^{-1}$) of 1–6 in Vacuo

	Taft–Kamlet ^a	Catalán3P ^b	Catalán4P	reaction field model ^c	Δ ^d
1 (abs)	30.11	30.21	29.93	29.79	0.43
1 (flu)	28.66	28.88	25.41	25.85	3.47
2 (abs)	28.89	29.09	28.49	28.66	0.60
2 (flu)	28.26	28.74	23.28	24.59	5.47
3 (abs)	29.16	29.27	27.67	28.40	1.61
3 (flu)	27.83	28.06	24.52	24.94	3.55
4 (abs)	27.32	27.49	27.05	27.10	0.44
4 (flu)	26.21	26.58	22.01	23.14	4.58
5 (abs)	30.05	31.12	31.09	30.68	1.07
5 (flu)	27.99	28.95	24.79	25.44	4.16
6 (abs)	31.44	32.14	32.67	31.84	1.22
6 (flu)	28.55	29.13	26.60	26.92	2.53

^aTransition energies in vacuo can be calculated by setting $\pi^* = -1.1$, and $\alpha = \beta = 0$ in the best-fit equations in the Taft–Kamlet model (Table 4).^{3d,15} ^bTransition energies in vacuo can be obtained directly by reading from ν_0 in their best-fit equations in the Catalán3P and Catalán4P models. ^cTransition energies determined by the reaction field model are imported from reference 1b. ^d Δ represents the maximum variation in the transition energies determined by different models.

$\times 10^3 \text{ cm}^{-1}$ is noticed for the fluorescence data. It is also interesting to note that the agreement between the Taft–Kamlet and Catalán3P models is considerably better, with average differences of 0.39 and 0.47 ($\times 10^3 \text{ cm}^{-1}$) for the absorption and fluorescence data, respectively. Similar consistency is also found between the Catalán4P and reaction field models, with average difference of 0.30 and 0.79 ($\times 10^3 \text{ cm}^{-1}$) for the absorption and fluorescence data, respectively. At the time of writing, we do not fully understand the root cause of this discrepancy.

3.3. Evaluation of the Solvatochromic Models for 1, 4, 5, and 7–12 Based on ν Determined from λ_{max} Criteria (Data Set B). The transition energies ν of this set of data are

derived by taking directly the reciprocal of λ_{max} . Furthermore, aromatic and polychlorinated solvents are included in these data (Table 1). Consequently, the associated transition energies in data set B contain higher noise than those of data set A, owing to the potential perturbations in bandgaps of coumarins when in different solvents. However, this simpler treatment to ν is a more popular choice than Moog's method, among all solvatochromic studies reported in the literature.^{9,17} The assessment based on this data set B can be thus considered as a “stability” test of the three solvatochromic models over various “noise” levels.

First, the best-fit equations to each solvatochromic model are determined based on the F -statistics (Supporting Information). The averaged goodness-of-fit parameters are summarized in Table 6. Both the Taft–Kamlet and the Catalán4P models

Table 6. Goodness-of-Fit (adj R^2) for the Statistical Best-Fit Equations in Empirical Solvatochromic Models

	Taft–Kamlet model	Catalán3P model	Catalán4P model
including data from all solvents	0.950	0.813	0.931
excluding data in aromatic and polychlorinated solvents	0.974	0.966	0.967

described the transition energy changes of coumarins relatively well, regardless of the types of solvents in use. In contrast, the Catalán3P model performs very poorly when data from polychlorinated solvents and aromatic solvents are included. Excluding these data dramatically improves the averaged adj R^2 for the Catalán3P model from 0.813 to 0.966 (Table 6). This exclusion leads only to a small increase in the goodness-of-fit parameters for the Taft–Kamlet and the Catalán4P models (~ 0.03 on average; Table 6). However, in some cases, this increase can be up to 0.09 (Supporting Information). Special care is thus required when applying aromatic and polychlorinated solvent data to all models, and it is recommended to perform best-fits to each type of solvents independently, provided that there are enough spectral data.

The different performance of these three models when dealing with aromatic and polychlorinated solvents can probably be rationalized by considering how their polarity scales are constructed. The π^* scale consists of an inhomogeneous mixing of solvent polarizability and dipolarity, while this mixing in the SPP scale is uniform (eq 10).^{6d} However, polarizability and polarity may carry different weights in the overall solvent effects, across different classes of solvents. The nonuniform mixing in π^* seems to work better. By separating polarizability and polarity into two terms, SP and SdP, the Catalán4P model also demonstrates good performance.

$$\text{SPP} = (0.49 \pm 0.03)\text{SP} + (0.38 \pm 0.01)\text{SdP} + (0.21 \pm 0.02) \quad (10)$$

In the statistically best-fit results (Supporting Information), there are again some unexpected terms, i.e., negative coefficients for nonexistent types of hydrogen-bond interactions. In total, there are six such terms among all 15 fitting equations in the Taft–Kamlet model, and three in the Catalán4P model. The Catalán3P model generates credible results only when aromatic and poly chlorinated solvents are excluded, in which case two invalid terms are nevertheless produced; we have set these coefficients to null. The revised best-fit equations based on actual solvent–solute interactions are summarized in Table 7. Best-fit

Table 7. Best-Fit Parameters ($\times 10^3 \text{ cm}^{-1}$) of the Empirical Solvatochromic Models for Data Set B^a

	Taft–Kamlet model ^b				Catalán3P model ^c				Catalán4P model					
	ν_0	s	a	b	adj R^2	ν_0	ϵ_{app}	ϵ_{sa}	ϵ_{sb}	adj R^2	C_{SP}	C_{SA}	C_{SB}	adj R^2
1 (abs)	28.55 (0.22)	-1.70 (0.35)	-1.17 (0.27)		0.916	30.44 (0.45)	-3.57 (0.57)	-2.05 (0.39)		0.971	-2.06 (1.63)	-1.62 (0.70)		0.888
1 (flu)	25.33 (0.25)	-2.44 (0.40)	-1.98 (0.31)		0.953	28.31 (0.93)	-5.61 (1.17)	-3.22 (0.80)		0.951	-1.90 (0.53)	-2.72 (1.06)		0.889
4 (abs)	25.30 (0.17)	-1.68 (0.29)	-0.79 (0.16)		0.954	27.80 (0.50)	-4.31 (0.63)	-0.95 (0.24)		0.980	-2.50 (1.03)	-0.92 (0.35)		0.947
4 (flu)	21.63 (0.59)	-2.21 (0.99)	-1.83 (0.55)		0.852	26.37 (1.24)	-7.94 (1.58)	-1.47 (0.61)		0.959	-2.58 (0.55)	-1.75 (0.66)		0.945
5 (abs)	28.80 (0.11)	-0.50 (0.26)		-3.03 (0.25)	0.991	30.62 (0.37)	-3.15 (0.59)	-0.81 (0.40)	-2.01 (0.34)	0.991	-2.08 (1.20)	-0.95 (0.47)	-2.17 (0.33)	0.991
5 (flu)	24.93 (0.22)	-2.81 (0.72)	-1.16 (0.58)	-2.41 (0.98)	0.987	28.90 (0.63)	-7.16 (1.00)	-1.71 (0.69)	-2.08 (0.58)	0.990	-2.46 (0.35)	-1.03 (0.70)	-2.90 (0.53)	0.989
7 (abs)	26.43 (0.25)	-1.63 (0.43)	-0.74 (0.24)		0.898	28.76 (0.67)	-4.04 (0.86)	-0.94 (0.33)		0.960	-2.71 (1.30)	-0.89 (0.44)		0.912
7 (flu)	22.48 (0.73)	-2.32 (1.23)	-1.80 (0.68)		0.790	28.07 (1.63)	-9.09 (2.08)	-1.24 (0.81)		0.939	-2.74 (0.75)	-1.62 (0.90)		0.905
8 (abs)	26.00 (0.20)	-1.63 (0.32)	-0.77 (0.18)		0.944	28.54 (0.51)	-4.33 (0.65)	-0.90 (0.25)		0.978	-2.32 (1.16)	-0.89 (0.38)		0.937
8 (flu)	21.99 (0.62)	-2.19 (1.04)	-1.59 (0.58)		0.810	27.23 (1.29)	-8.46 (1.64)	-1.12 (0.64)		0.954	-2.38 (0.77)	-1.49 (0.92)		0.876
9 (abs)	28.16 (0.20)	-1.74 (0.32)	-1.00 (0.24)		0.923	30.14 (0.46)	-3.66 (0.58)	-1.82 (0.40)		0.968	-2.55 (1.37)	-1.37 (0.59)		0.912
9 (flu)	25.03 (0.28)	-2.62 (0.45)	-1.87 (0.35)		0.942	28.46 (0.99)	-6.20 (1.24)	-3.16 (0.85)		0.950	-2.00 (0.62)	-2.48 (1.23)		0.854
10 (abs)	25.97 (0.15)	-1.74 (0.24)	-0.62 (0.18)		0.953	28.27 (0.29)	-4.08 (0.37)	-0.72 (0.21)		0.988	-2.31 (0.87)	-0.66 (0.33)		0.958
11 (abs)	24.03 (0.13)	-1.04 (0.20)	-0.58 (0.15)		0.931	25.24 (0.42)	-2.18 (0.53)	-0.91 (0.30)		0.946	-1.92 (0.72)	-0.86 (0.27)		0.939
12 (abs)	29.51 (0.20)	-1.12 (0.32)	-0.75 (0.27)	-1.12 (0.39)	0.954	31.08 (0.79)	-2.67 (1.19)	-1.31 (0.55)	-1.10 (0.68)	0.943	-2.36 (1.28)	-1.27 (0.49)	-1.18 (0.45)	0.942
mean					0.920					0.964				0.926

^aThe numbers in parentheses represent 95% confidence limits for their corresponding fitting coefficients. ^bThe best-fit parameters in the Taft–Kamlet and Catalán4P models are computed based on spectral data collected in all different solvents. ^cFor the calculations of best-fit parameters in the Catalán3P model, data from aromatic and chlorinated solvents are excluded.

equations excluding data from aromatic and polychlorinated solvents are close to those reported in this table for both the Taft–Kamlet and Catalán4P models (Supporting Information).

We have also assessed the impact of different choices of Taft–Kamlet solvent parameters on the statistical fitting results, i.e., using both our method and Moog's selection of Taft–Kamlet solvent parameters. It has been demonstrated that both choices afford similar best-fit results and goodness-of-fit parameters (Supporting Information).

A crosscheck of the best-fitting parameters of **1**, **4**, and **5** from both data sets A and B show that their results are similar in general, except of the best-fits for the fluorescence data of **4**. It is interesting to note that the best-fit of **4** in data set B possesses a relatively low adj R^2 and appears less reliable; when data from aromatic and polychlorinated solvents are excluded, adj R^2 of the resulting best-fit improves from 0.852 to 0.936, and the new best-fit equation has a better agreement with that in data set A (Supporting Information). Overall, however, the decent agreement between best-fitting parameters both from data sets A and B suggests that the perturbations in bandgaps of coumarins when in different solvents are relatively small, and using the reciprocal of λ_{\max} directly to calculate ν is a reasonable choice, although less ideal than Moog's treatment or other more sophisticated fittings. One can thus make use of the fitting results both in Tables S4 (Supporting Information; a revised version of Table 2) and 7 and draw some interesting conclusions.

First, type C hydrogen bonds play a more important role than type B hydrogen bonds in the red shifting of coumarins. In the Taft–Kamlet model, the ratios between s , a , and b measure the relative contributions of their associated solvent properties upon a change in ν .^{3d} In the fitting equations to the absorption data of **5** and **6** (Table S4 and Table 7), each of which have two HBD moieties, b is significantly larger than a and s (to the extent that a is rendered statistically insignificant in the case of **5**). For **12**, there is only one HBD moiety. The relative weight of b decreases, but it is still larger than that of a (Table 7).

This critical effect of type C hydrogen bonds is justified by quantum mechanical/molecular mechanical calculations. For example, Sakata et al. have calculated the absorption spectrum of **6** in water; they concluded that the solvent structure around the amino group of **6**, i.e., the $\text{NH}\cdots\text{O}$ interactions (type C hydrogen bonds), plays a key role to the red shifting of its spectra.¹⁸

Second, it is noted that the absorption spectral shift in the Catalán4P model is sensitive to both solvent polarizability and dipolarity in all but one case. The one exception, the fitting equation to the absorption data of **3**, displays the lowest adj R^2 in data set A and is least convincing. In contrast, the fluorescence spectral shift is only sensitive to dipolarity among the nonspecific solvent effects for all coumarins; the effect from polarizability is statistically insignificant.

The relatively more important role of solvent dipolarity manifesting in emission than in absorption is understandable. Only during the emission process do solvent molecules around coumarins have enough time to reorganize themselves in order to align with excited polar coumarins.¹⁹ This better alignment leads to more effective dipole–dipole interactions between coumarins and solvents, and causes an enhanced stabilization effect that decreases the energy levels of excited coumarins to yield a larger red shift.

The Catalán4P model offers insights on different roles of solvent dipolarity and polarizability on coumarin spectral shifts. However, it is obvious that with one additional parameter in the Catalán4P model in comparison to the Taft–Kamlet and

Catalán3P models, more spectral data are required for a reliable fit in the former model; when only a limited sample size of such data is available (i.e., ~ 10), using the latter two models is more justifiable.

In summary, all three empirical models demonstrate excellent statistical performance in describing the solvatochromism of coumarins, when aromatic and polychlorinated solvents are excluded. As these solvents are included with other aliphatic solvents, the adj R^2 parameters decrease marginally for both the Taft–Kamlet and Catalán4P model; and the Catalán3P model fails to accurately model the spectral shifts of coumarins in such a case. Furthermore, the best-fit coefficients of these models allow one to appreciate the importance of different aspects of solvent effects, and gain a deeper insight into the nature of the solvent–coumarin interactions. However, it is important not to overinterpret purely statistical results. Physical validation of the best-fit results, based on the molecular structures of both solvents and solutes and their corresponding interactions, are essential in order to determine a valid best-fit equation for all three empirical models.

3.4. Solvatochromism of 13 (Data Set C). It should be pointed out that specific solvent effects are not limited to hydrogen-bond interactions. There are other types of interactions, such as probe–probe interactions (i.e., forming excited dimers), acid–base chemistry (electron-pair donor/electron-pair acceptor interactions), preferential solvation (in mixed solvents), varied excitation mechanisms (i.e., changing from local excited emission to ICT induced emission as solvent polarity changes, i.e., altering bandgap shapes), and significant conformational changes.^{2,19} While solvatochromic studies assume complete solvation of solutes, aggregation is possible for some compounds, even at low concentration. Consequently, when the spectral data do not fit to an empirical solvatochromic model well, it is not necessarily a failure of the model, but often an indication of unaccounted effects; the solvatochromism of **13** is used to illustrate one such effect.

By directly dissolving **13** into ten different (nonaromatic and nonchlorinated) solvents, the respective λ_{\max} values were used to calculate ν for fitting into the Taft–Kamlet model (data set C; Supporting Information). The resulting best-fit (eq 11) has a surprisingly low adj R^2 of only 0.550, unlike other coumarin derivatives. (Low adj R^2 is also observed in the Catalán3P model and the sample size is too small for a credible fitting via the Catalán4P model.)

$$\nu = (23.98 \pm 0.67) - (0.91 \pm 0.93)\pi^* + (0.61 \pm 0.71)\alpha - (1.45 \pm 1.27)\beta \quad (11)$$

Auxiliary research shows that serious molecular aggregation of **13**, when in solvents, such as cyclohexane, could occur even at low concentration.²⁰ Its UV–vis absorption peak had been shown to shift from 405.8 to 430.0 nm as its concentration in cyclohexane solution increases from 10^{-7} to 3×10^{-6} M, due to the increasing levels of molecular aggregation.^{20a} Correa et al. noticed this and consequently measured the UV–vis absorption of **13** in 14 solvents, carefully selecting only peaks/shoulders that were representative of monomers of **13** for deducing a best-fit of the data to the Taft–Kamlet model. This led to a new best-fit equation with a correlation coefficient as high as 0.98 (eq 12).^{20a}

$$\nu = (24.29 \pm 0.06) - (0.53 \pm 0.09)\pi^* + (0.21 \pm 0.10)\alpha - (1.61 \pm 0.20)\beta \quad (12)$$

However, a scrutiny of the hydrogen-bond interactions of **13** with various solvents shows that this equation is still problematic. First, when molecules of **13** interact with HBD solvents, type B hydrogen bonds play a more important role than type A hydrogen bonds, and such interactions result in a red shift (i.e., a reduction in transition energy). Indeed, the coefficients of α in the best-fits of **1–12** are either negative or null, i.e., statistically insignificant (Tables S4 and 7). In contrast, this coefficient is positive in eq 12. Second, when TD-DFT calculations are used to emulate the type D hydrogen bonds in **13**, (i.e., by explicitly placing an ethanol/DMSO molecule near the H atom in the $-\text{COOH}$ group of **13**), the resultant hydrogen bonds are predicted to produce a blue shift of up to ~ 5 nm.^{20b} One would therefore anticipate that the coefficient of β should be positive; yet, it is negative in eq 12.

A more detailed investigation of this discrepancy reveals that the molecular conformation of **13** may present a significant change when engulfed in HBA solvents.^{20b} For example, in non-HBA solvents, the $-\text{COOH}$ group in **13** forms an intramolecular hydrogen bond with its carbonyl oxygen, and the H atom in $-\text{COOH}$ does not possess good contact with solvent molecules, owing to its bond geometry. Nevertheless, this bond can be “opened up” in HBA solvents, leading to intensive hydrogen-bond interactions. Moreover, there is more than one type of aggregation phase for **13** when present in nonpolar solvents. Hence, the UV–vis spectra of **13** essentially consist of signals from its different molecular conformations, and possible types and levels of molecular aggregation. The anomalous fitting coefficients in eq 12 could very well result from such “intrinsic contamination” to the λ_{max} data.

4. CONCLUSIONS

The $\lambda_{\text{max}}^{\text{abs}}$ values of **10–12** (coumarins 314T, 445, and 522B) in 17 different solvents have been reported herein, while this information for an additional 10 coumarins were extracted from the literature. These data are used to understand the solvent effects on the spectral shift of the coumarin dyes and evaluate the performance of three empirical solvatochromic models: the popular Taft–Kamlet model and two more recent Catalán models. It has been demonstrated that all three models offer very good statistical performance for aliphatic solvents. However, owing to the considerably different polarizability of aromatic and polychlorinated solvents (with respect to aliphatic solvents), the overall goodness-of-fit of coumarin data to these models decreases when these solvents are included in the solvatochromic fitted data. This decrease is marginal for the Taft–Kamlet and Catalán4P models but significant for the Catalán3P model.

It is also shown that the statistically best-fits to all three models can carry invalid parameters, corresponding to physically nonexistent types of solvent–solute interactions. It is important to always validate the best-fitting results (i.e., setting the invalid coefficients to null), based on the molecular structures of both solutes and solvents and their corresponding hydrogen-bond interactions. Upon such validations, the goodness-of-fit of the resulting best-fits remain high and their parameters are physically valid. Considering the validated best-fit parameters, we notice that among nonspecific solvent effects, dipolarity plays a more critical role in the red shifting of the fluorescence spectra than in absorption spectra of coumarins, and among specific solvent effects, the effect from type C hydrogen bonds is the most significant.

Lastly, we demonstrate that the “failure” of empirical solvatochromic models in accurately describing the spectral

shift of **13** (coumarin 343) in terms of low goodness-of-fit, or the “invalidity” in the resultant fitting parameters, provide useful hints about the presence of other types of solvent–solute interactions, such as significant conformational changes and molecular dye aggregation. This is illustrated in more detail via a companion paper.^{20b}

In summary, empirical solvatochromic models provide valuable information on solvents effects and shed light on the exact structures of solute molecules in the solution phase. The results reported herein are highly relevant to solvent effect investigations of all sorts of organic compounds that employ empirical solvatochromic models.

■ ASSOCIATED CONTENT

Supporting Information

Solvent properties defined in empirical solvatochromic models, the UV–vis absorption/fluorescence spectral data of **1–13**, the revised best-fit parameters of data set A, and the best-fit parameters of data set B in different scenarios (i.e., including or excluding data in aromatic and polychlorinated solvents). This material is available free of charge via the Internet at <http://pubs.acs.org>.

■ AUTHOR INFORMATION

Corresponding Author

*E-mail: jmc61@cam.ac.uk. Tel: +44 (0)1223 337470. Fax: +44 (0)1223 373536.

Notes

The authors declare no competing financial interest.

■ ACKNOWLEDGMENTS

The authors thank Dr. Paul Waddell from the Department of Physics, University of Cambridge, U.K., for his helpful comments on this manuscript. X.L. is indebted to the Singapore Economic Development Board for a Clean Energy Scholarship. K.S.L. acknowledges the EPSRC for a DTA Ph.D. studentship (EP/P504120/1). J.M.C. thanks the Royal Society for a University Research Fellowship, the University of New Brunswick (UNB), Canada, for The UNB Vice-Chancellor’s Research Chair and NSERC for the Discovery Grant, 355708.

■ REFERENCES

- (1) (a) Moog, R. S.; Davis, W. W.; Ostrowski, S. G.; Wilson, G. L. Solvent Effects on Electronic Transitions in Several Coumarins. *Chem. Phys. Lett.* **1999**, *299*, 265–271. (b) Moog, R. S.; Kim, D. D.; Oberle, J. J.; Ostrowski, S. G. Solvent Effects on Electronic Transitions of Highly Dipolar Dyes: a Comparison of Three Approaches. *J. Phys. Chem. A* **2004**, *108*, 9294–9301. (c) Aaron, J.-J.; Buna, M.; Parkanyi, C.; Antonious, M. S.; Tine, A.; Cisse, L. Quantitative Treatment of the Effect of Solvent on the Electronic Absorption and Fluorescence Spectra of Substituted Coumarins: Evaluation of the First Excited Singlet-state Dipole Moments. *J. Fluoresc.* **1995**, *5*, 337–347. (d) Raikar, U. S.; Tangod, V. B.; Mannopantar, S. R.; Mastiholi, B. M. Ground and Excited State Dipole Moments of Coumarin 337 Laser Dye. *Opt. Commun.* **2010**, *283*, 4289–4292. (e) Nad, S.; Pal, H. Unusual Photophysical Properties of Coumarin 151. *J. Phys. Chem. A* **2001**, *105*, 1097–1106. (f) Nad, S.; Kumbhakar, M.; Pal, H. Photophysical Properties of Coumarin 152 and Coumarin 481 Dyes: Unusual Behavior in Nonpolar and in Higher Polarity Solvents. *J. Phys. Chem. A* **2003**, *107*, 4808–4816. (g) Nad, S.; Pal, H. Photophysical Properties of Coumarin-500 (C500): Unusual Behavior in Nonpolar Solvents. *J. Phys. Chem. A* **2003**, *107*, 501–507. (h) Pal, H.; Nad, S.; Kumbhakar, M. Photophysical Properties of Coumarin 120: Unusual Behavior in Nonpolar Solvents. *J. Chem. Phys.* **2003**, *119*, 443–452. (i) Das, K.; Jain, B.; Patel, H. S. Hydrogen

Bonding Properties of Coumarin 151, 500, and 35: the Effect of Substitution at the 7-amino Position. *J. Phys. Chem. A* **2006**, *110*, 1698–1704.

(2) Reichardt, C.; Welton, T. *Solvents and Solvent Effects in Organic Chemistry*; Wiley-VCH: Weinheim, Germany, 2011.

(3) (a) Kamlet, M. J.; Taft, R. The Solvatochromic Comparison Method. I. The β -Scale of Solvent Hydrogen-bond Acceptor (HBA) Basicities. *J. Am. Chem. Soc.* **1976**, *98*, 377–383. (b) Taft, R.; Kamlet, M. J. The Solvatochromic Comparison Method. 2. The Alpha-Scale of Solvent Hydrogen-bond Donor (HBD) Acidities. *J. Am. Chem. Soc.* **1976**, *98*, 2886–2894. (c) Kamlet, M. J.; Abboud, J. L.; Taft, R. The Solvatochromic Comparison Method. 6. The π^* Scale of Solvent Polarities. *J. Am. Chem. Soc.* **1977**, *99*, 6027–6038. (d) Kamlet, M. J.; Abboud, J. L. M.; Abraham, M. H.; Taft, R. Linear Solvation Energy Relationships. 23. A Comprehensive Collection of the Solvatochromic Parameters, π^* , α , and β , and Some Methods for Simplifying the Generalized Solvatochromic Equation. *J. Org. Chem.* **1983**, *48*, 2877–2887.

(4) (a) Ooshika, Y. Absorption Spectra of Dyes in Solution. *J. Phys. Soc. Jpn.* **1964**, *9*, 594–602. (b) Lippert, E. Dipolmoment und Elektronenstruktur von Angeregten Molekülen. *Z. Naturforsch.* **1955**, *109*, 541–545. (c) Horng, M. L.; Gardecki, J. A.; Papazyan, A.; Maroncelli, M. Subpicosecond Measurements of Polar Solvation Dynamics: Coumarin 153 Revisited. *J. Phys. Chem.* **1995**, *99*, 17311–17337. (d) McRae, E. G. Theory of Solvent Effects on Molecular Electronic Spectra. Frequency Shifts. *J. Phys. Chem.* **1957**, *61*, 562–572. (e) Mataga, N.; Kaifu, Y.; Koizumi, M. The Solvent Effect on Fluorescence Spectrum, Change of Solute-solvent Interaction During the Lifetime of Excited Solute Molecule. *Bull. Chem. Soc. Jpn.* **1955**, *28*, 690–691.

(5) Reichardt, C. Solvatochromic Dyes as Solvent Polarity Indicators. *Chem. Rev.* **1994**, *94*, 2319–2358.

(6) (a) Catalán, J.; López, V.; Pérez, P.; Martín-Villamil, R.; Rodríguez, J. G. Progress Towards a Generalized Solvent Polarity Scale: the Solvatochromism of 2-(Dimethylamino)-7-nitrofluorene and Its Homomorph 2-fluoro-7-nitrofluorene. *Liebigs Annalen* **1995**, *1995*, 241–252. (b) Catalán, J.; Díaz, C.; López, V.; Pérez, P.; De Paz, J. L. G.; Rodríguez, J. G. A Generalized Solvent Basicity Scale: the Solvatochromism of 5-nitroindoline and Its Homomorph 1-methyl-5-nitroindoline. *Liebigs Annalen* **1996**, *1996*, 1785–1794. (c) Catalán, J.; Díaz, C. A Generalized Solvent Acidity Scale: The Solvatochromism of o-tert-Butylstilbazolium Betaine Dye and Its Homomorph O,O'-Di-tert-butylstilbazolium Betaine Dye. *Liebigs Annalen* **1997**, *1997*, 1941–1949. (d) Catalán, J. Toward a Generalized Treatment of the Solvent Effect Based on Four Empirical Scales: Dipolarity (SdP, a new scale), Polarizability (SP), Acidity (SA), and Basicity (SB) of the Medium. *J. Phys. Chem. B* **2009**, *113*, 5951–5960.

(7) (a) Catalán, J. On the π^* Solvent Scale. *J. Org. Chem.* **1995**, *60*, 8315–8317. (b) Drago, R. S. Extension of the Unified Scale of Solvent Polarities to Acceptor Probes: Concerns about β - π^* Parameters. *J. Org. Chem.* **1992**, *57*, 6547–6552.

(8) Abe, T. Improvements of the Empirical π^* Solvent Polarity Scale. *Bull. Chem. Soc. Jpn.* **1990**, *63*, 2328–2338.

(9) Filarowski, A.; Kluba, M.; Cieřlik-Boczula, K.; Koll, A.; Kochel, A.; Pandey, L.; De Borggraeve, W. M.; Van der Auweraer, M.; Catalán, J.; Boens, N. Generalized Solvent Scales as a Tool for Investigating Solvent Dependence of Spectroscopic and Kinetic Parameters. Application to Fluorescent Bodipy Dyes. *Photochem. Photobiol. Sci.* **2010**, *9*, 996–1008.

(10) (a) Husain, M. M.; Sindhu, R.; Tandon, H. C. Photophysical Properties and Estimation of Ground and Excited State Dipole Moments of 7-diethylamino and 7-diethylamino-4-methyl Coumarin Dyes from Absorption and Emission Spectra. *Eur. J. Chem.* **2012**, *3*, 87–93. (b) Jones, G., II; Jackson, W. R.; Kanoktanaporn, S.; Halpern, A. M. Solvent Effects on Photophysical Parameters for Coumarin Laser Dyes. *Opt. Commun.* **1980**, *33*, 315–320.

(11) (a) McCarthy, P. K.; Blanchard, G. J. AM1 Study of the Electronic Structure of Coumarins. *J. Phys. Chem.* **1993**, *97*, 12205–12209. (b) Cave, R. J.; Castner, E. W., Jr. Time-dependent Density Functional

Theory Investigation of the Ground and Excited States of Coumarins 102, 152, 153, and 343. *J. Phys. Chem. A* **2002**, *106*, 12117–12123.

(12) (a) Zhao, W.; Pan, L.; Bian, W.; Wang, J. Influence of Solvent Polarity and Hydrogen Bonding on the Electronic Transition of Coumarin 120: a TDDFT Study. *ChemPhysChem* **2008**, *9*, 1593–1602. (b) Kamlet, M. J.; Dickinson, C.; Taft, R. Linear Solvation Energy Relationships: Solvent Effects on Some Fluorescence Probes. *Chem. Phys. Lett.* **1981**, *77*, 69–72.

(13) Marcus, Y. The Properties of Organic Liquids That Are Relevant to Their Use as Solvating Solvents. *Chem. Soc. Rev.* **1993**, *22*, 409–416.

(14) Laurence, C.; Nicolet, P.; Dalati, M. T.; Abboud, J. L. M.; Notario, R. The Empirical Treatment of Solvent-Solute Interactions: 15 Years of π^* . *J. Phys. Chem.* **1994**, *98*, 5807–5816.

(15) Abboud, J. L. M.; Notario, R. Critical Compilation of Scales of Solvent Parameters. Part I. Pure, Non-hydrogen Bond Donor Solvents. *Pure Appl. Chem.* **1999**, *71*, 645–718.

(16) By using Moog's choice of Taft–Kamlet solvent parameters, the average adj R^2 is slightly better, amounted to 0.985.

(17) Effenberger, F.; Wuerthner, F.; Steybe, F. Synthesis and Solvatochromic Properties of Donor-Acceptor-Substituted Oligothiophenes. *J. Org. Chem.* **1995**, *60*, 2082–2091.

(18) Sakata, T.; Kawashima, Y.; Nakano, H. Solvent Effect on the Absorption Spectra of Coumarin 120 in Water: a Combined Quantum Mechanical and Molecular Mechanical Study. *J. Chem. Phys.* **2011**, *134*, 014501.

(19) Lakowicz, J. R. *Principles of Fluorescence Spectroscopy*; Springer: New York, 2006.

(20) (a) Correa, N. M.; Levinger, N. E. What Can You Learn from a Molecular Probe? New Insights on the Behavior of C343 in Homogeneous Solutions and AOT Reverse Micelles. *J. Phys. Chem. B* **2006**, *110*, 13050–13061. (b) Liu, X.; Cole, J. M.; Low, K. S. Molecular Origins of Dye Aggregation and Complex Formation Effects in Coumarin 343. *J. Phys. Chem. C* **2013**, *117*, 10.1021/jp4024266.